

Nonlinear Position Control of a Very Flexible Parallel Robot Manipulator

Peter Eberhard and Fatemeh Ansarieshlaghi

Abstract In this paper, we investigate the control of a very flexible parallel robot with high accuracy. This robot has two very flexible long links and can be modeled as an underactuated multibody system since it has fewer control inputs than degrees of freedom for rigid body motion and deformation. Therefore, these flexibilities are taken into account in the control design. In order to obtain high performance in the end-effector trajectory tracking, an accurate and efficient nonlinear controller is designed. This nonlinear feedback controller is based on the Lyapunov approach using the measurable states of the system. Then, it is carefully tested on the flexible parallel robot. The simulation and experimental results show that the end-effector tracks desired trajectories with high accuracy. Also, the designed controller is compared to previous works and the results show that the controller can achieve higher tracking performance.

1 Introduction

Light-weight manipulators attract a lot of research interest because of their complementing advantages. The advantages of light-weight robots include low energy usage, less mass, and often high working speeds. However, due to the light-weight design, the bodies have a significant flexibility which yields undesired deformations and vibrations. Therefore, this manipulator is modeled as a flexible multibody system and the flexibilities must be taken into account in the control design. The flexible system with significant deformations complicates the control design because there are more generalized coordinates than control inputs. In order to obtain high performance in the end-effector trajectory tracking of a flexible manipulator, an accurate

Peter Eberhard · Fatemeh Ansarieshlaghi
Institute of Engineering and Computational Mechanics, University of Stuttgart
Pfaffenwaldring 9, 70569 Stuttgart, Germany
e-mail: {peter.eberhard, fatemeh.ansari}@itm.uni-stuttgart.de

and efficient nonlinear feedforward and feedback controller are advantageous. The difficulty of designing a nonlinear feedback controller with high performance for a highly flexible system is increased, when the controller does not have access to direct measurement of the end-effector and all the system states. To overcome this problem, the system model can be reduced based on the system constraints. Finally, based on the reduced model of the system, a nonlinear feedback controller can be designed.

To investigate a flexible manipulator here, a lambda shape robot is used. In previous works on the lambda robot, some linear controllers and a nonlinear feedback controller were designed based on the system model. The linear controllers were designed using the measurable system states [6,9]. Also, a nonlinear controller was designed based on the feedback linearization approach and all the estimated states were obtained by a nonlinear observer [2].

The novelty of this work is, that a nonlinear feedback controller for high-speed trajectory tracking of a very flexible parallel lambda robot is designed. This controller is based on the reduced model of the system and the direct method of Lyapunov [8] using the measurable system states. Using the reduced model of the system and only measurable states, there is no need to observe and estimate all the system states. Therefore, in this method, the corresponding estimation error is removed.

In this paper, the nonlinear feedback controller is implemented on the simulated model of a very flexible parallel robot and tested on the real system. The results show that the end-effector tracks a trajectory with high performance and higher accuracy compared to the previous works.

The paper is organized as follows: Section 2 describes the robot and Section 3 includes the modeling of the flexible parallel lambda robot. Section 4 explains the architecture of the nonlinear controller. In Section 5, the proposed nonlinear controller is simulated and tested on the robot and the results are discussed.

2 Flexible Lambda Robot

The used lambda robot is a simple parallel robot manipulator. This robot has highly flexible links. The end of the short link is connected in the middle of the long link using rigid bodies. This connection creates a closed loop kinematics constraint that causes the parallel configuration of the robot. This robot has two prismatic actuators connecting the links to the ground. The links are connected using passive revolute joints to the linear actuators. Another revolute joint is used to connect the short link and the middle of the long link. An additional rigid body is attached to the free end of the long link as an end-effector. The drive positions and velocities are measured with two optical encoders. Three full Wheatstone bridge strain gauge sets are attached on the long flexible link to measure its deformation. The lambda robot configuration is shown in Figure 1 has been built in hardware, see [6] at the Institute of Engineering and Computational Mechanics of the University of Stuttgart.

The electrical part of the hardware includes some power supplies for motors, strain gauge's amplifiers, digital/analog input-outputs boards, one *Speedgoat* target, a host computer, etc. For controlling the robot, the online control is done with a *Speedgoat* performance real-time target machine running a *Mathworks xPCtarget* kernel, which is called *Simulink Real-Time* since *Matlab R2014a*. Also, to observe the controller progress a graphical user interface is available for the input, output, safety logic of the lambda robot and the communication.

3 Modeling of the Flexible Lambda Robot

The modeling process of the flexible manipulator with λ configuration can be separated into three major steps. First, the flexible components of the system are modeled with the linear finite element method in the commercial finite element code *ANSYS*. Next, in order to control the λ robot, the degrees of freedom of the flexible bodies shall be decreased. Therefore, model order reduction is utilized. Then, all the rigid and flexible parts are modeled as a multibody system with a kinematic loop. The equation of motion with a kinematic loop constraint of the flexible parallel manipulator using the generalized coordinates $\mathbf{q} \in \mathbf{R}^5$ is

$$\mathbf{M}(\mathbf{q})\ddot{\mathbf{q}} + \mathbf{k}(\mathbf{q}, \dot{\mathbf{q}}) = \mathbf{g}(\mathbf{q}, \dot{\mathbf{q}}) + \mathbf{B}(\mathbf{q})\mathbf{u} + \mathbf{C}^T(\mathbf{q})\boldsymbol{\lambda} , \quad (1a)$$

$$\mathbf{c}(\mathbf{q}) = \mathbf{0} . \quad (1b)$$

The symmetric, positive definite mass matrix $\mathbf{M} \in \mathbf{R}^{5 \times 5}$ depends on the joint angles and the elastic coordinates. The vector $\mathbf{k} \in \mathbf{R}^5$ contains the generalized centrifugal, Coriolis and Euler forces, and $\mathbf{g} \in \mathbf{R}^5$ includes the vector of applied forces and inner forces due to the body elasticity. The input matrix $\mathbf{B} \in \mathbf{R}^{5 \times 2}$ maps the input vector $\mathbf{u} \in \mathbf{R}^2$ to the system. The constraint equations are defined by $\mathbf{c} \in \mathbf{R}^2$. The Jacobian matrix of the constraint $\mathbf{C} = \partial(\mathbf{c}(\mathbf{q}))/\partial\mathbf{q} \in \mathbf{R}^{2 \times 5}$ maps the reaction force $\boldsymbol{\lambda} \in \mathbf{R}^2$ due to the kinematic loop. The flexible lambda robot in hardware and its mechanical model are shown in Figure 1 left, see also [1, 3, 6].

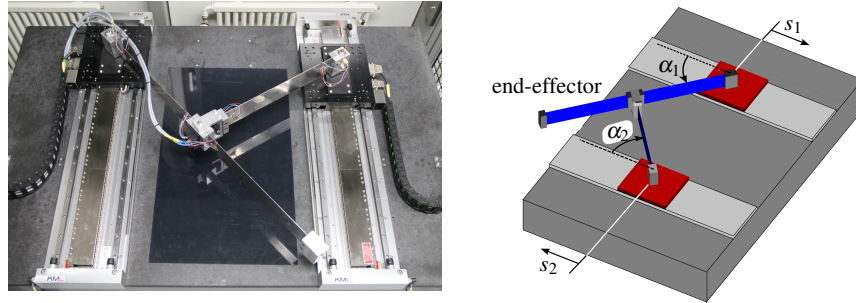


Fig. 1 Lambda robot, mechanical setup of the robot and simulation model of flexible parallel robot.

While the system has a kinematics loop as a constraint, the system coordinates derivative $\dot{\mathbf{q}}$ can be divided to dependent $\dot{\mathbf{q}}_d$ and independent $\dot{\mathbf{q}}_i$ coordinates and the system constraints can be written as

$$\ddot{\mathbf{c}} = \mathbf{C}\ddot{\mathbf{q}} + \mathbf{c}'' = \mathbf{C}_i\ddot{\mathbf{q}}_i + \mathbf{C}_d\ddot{\mathbf{q}}_d + \mathbf{c}'', \quad (2)$$

where \mathbf{C}_d and \mathbf{C}_i are dependent and independent parts of the Jacobian matrix of the constraint and \mathbf{c}'' presents local accelerations due to the constraints. Based on Equation (2), the system coordinates can be formulated by

$$\ddot{\mathbf{q}} = \begin{bmatrix} \ddot{\mathbf{q}}_i \\ \ddot{\mathbf{q}}_d \end{bmatrix} = \begin{bmatrix} \mathbf{I}_{3 \times 3} \\ -\mathbf{C}_d^{-1}\mathbf{C}_i \end{bmatrix} \ddot{\mathbf{q}}_i + \begin{bmatrix} \mathbf{0}_{3 \times 3} \\ -\mathbf{C}_d^{-1}\mathbf{c}'' \end{bmatrix} = \mathbf{J}_c\ddot{\mathbf{q}}_i + \mathbf{b}'' \quad (3)$$

Finally, by left-side multiplication with the transposed of the Jacobian matrix \mathbf{J}_c and replacing $\ddot{\mathbf{q}}$ by Equation (3), the equation of motion (1a) can be determined, see [4,5], by

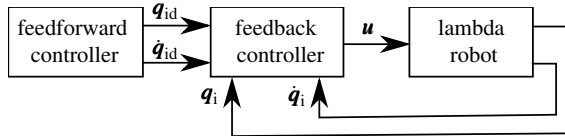
$$\bar{\mathbf{M}}\ddot{\mathbf{q}}_i = -\bar{\mathbf{k}} + \bar{\mathbf{g}} + \bar{\mathbf{B}}\mathbf{u} = \bar{\mathbf{f}} + \bar{\mathbf{B}}\mathbf{u}. \quad (4)$$

The new dynamics formulation of the lambda robot, Equation (4), based on the independent states of the system is named the reduced model.

4 Control of the Flexible Lambda Robot

The lambda robot control is separated into feedforward and feedback control parts. The designed nonlinear controller structure is shown in Figure 2.

Fig. 2 Nonlinear feedback controller structure.



In the feedforward control part, the offline part, the desired trajectories of the system states (\mathbf{q}_{id} , $\dot{\mathbf{q}}_{id}$) are calculated using a two-point boundary value problem based on the desired end-effector trajectory. The two-point boundary value problem is used while the flexible multibody system is a non-minimum phase system with internal dynamics [5]. The feedback control part computes the lambda robot input (\mathbf{u}) using the reduced nonlinear dynamics of the robot in Equation (4), the measured states (\mathbf{q}_i , $\dot{\mathbf{q}}_i$), and the desired states based on the direct method of Lyapunov [8] in real-time. This controller is named reduced nonlinear feedback controller.

To design a nonlinear feedback controller for the system in Equation (4), the control law is obtained for the lambda robot as

$$\mathbf{u} = \bar{\mathbf{B}}^{-1}(-\bar{\mathbf{f}} + \bar{\mathbf{M}}(\mathbf{K}_p\mathbf{e} + \mathbf{K}_D\dot{\mathbf{e}})), \quad (5)$$

where \mathbf{q}_{id} is the desired value for \mathbf{q}_i , consequently $\dot{\mathbf{q}}_{id}$ is the desired value for $\dot{\mathbf{q}}_i$ and the error and the dynamics of error are calculated by $\mathbf{e} = \mathbf{q}_i - \mathbf{q}_{id}$ and $\dot{\mathbf{e}} = \dot{\mathbf{q}}_i - \dot{\mathbf{q}}_{id}$. The desired values depend on the desired trajectory of the end-effector and can be computed via the feedforward part and \mathbf{q}_{id} and $\dot{\mathbf{q}}_{id}$ can be set. The matrices \mathbf{K}_P and \mathbf{K}_D correspond to the weighting of feedback errors and can be designed via the LQR method or tuned by hand. Also, they should satisfy the stability conditions for nonautonomous systems as a uniform stability, based on the Lyapunov theorem. The inverse of the input matrix $\bar{\mathbf{B}}$ is not so straightforward to calculate, since it is not of full row rank. Therefore, the existing left-inverse is used as a pseudo-inverse to yield $\bar{\mathbf{B}}\bar{\mathbf{B}}^{-1} = \mathbf{I}$. The vector \mathbf{u} presents the control input of the robot manipulator and that is the output of the designed position controller based on the Lyapunov method.

5 Simulation and Experimental Results

The controller is tested in real-time on the machine with 250 μs sampling time. Therefore, the camera with image processing is not applicable for online tracking the end-effector position and it can be used only for offline validation. To validate the designed nonlinear feedback controller, the end-effector tracks a trajectory and a camera records the movie during the trajectory tracking. Then, the recorded movie is used for offline validation.

To track the end-effector position and transfer the recorded movie from pixel to meter, two light points are attached to the end-effector with specified distance. Figure 3 shows these light points on the end-effector and the offline image processing results of the light points that are recorded by the camera during tracking a line trajectory. Also, the position of the camera is fixed and the camera view for each point of the trajectories are different. Hence, camera calibration is required. For this goal, a checkerboard is used for the calibration in [7]. The camera parameters are used to correct an image for lens distortion. Then, the corrected images are used for tracking the two light points on the end-effector.

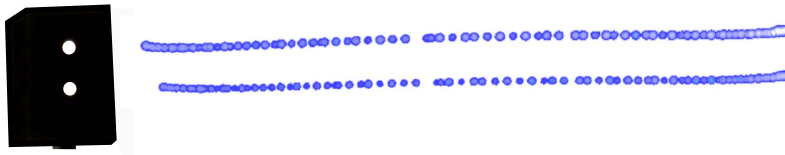


Fig. 3 End-effector and the light points (left), offline image processing result for the recorded movie of the end-effector position (right).

The CPU time to calculate the system input based on the system dynamics model, the measurements, and desired signals is less than 100 μs . That means that the total

CPU time for the running controller loop and getting the measurements is less than sampling time. Thus, the controller fits for the real-time test.

In order to investigate the controller performance, the robot based on the designed nonlinear controller tracks two different trajectories with different velocities as test scenarios. Also, the tracking performance of the robot's end-effector is compared with the previous work. Hence, the presented nonlinear feedback controller in Equation (5) (named the reduced nonlinear controller) and the feedback controller in [2] (named the nonlinear controller) are implemented on the lambda robot in simulation and tested on the real system. Also, the end-effector trajectory tracking error and the strain of the long flexible link are chosen as comparison benchmarks.

The first scenario is a line tracking task. The goal of this scenario is to validate the tracking performance in high-speed motion and investigate the end-point error. To this end, the robot end-effector shall track a line with length 0.283 m and with a maximum velocity of 1.2374 m/s . The end-effector based on the controllers tracks a line with the start point $x_s = [-0.6, -0.5]^T\text{ m}$ and the end point $x_e = [-0.8, -0.3]^T\text{ m}$. The movie in this scenario is recorded with approximately 300 frame per second. The simulation and experiment results are shown in Figure 4.

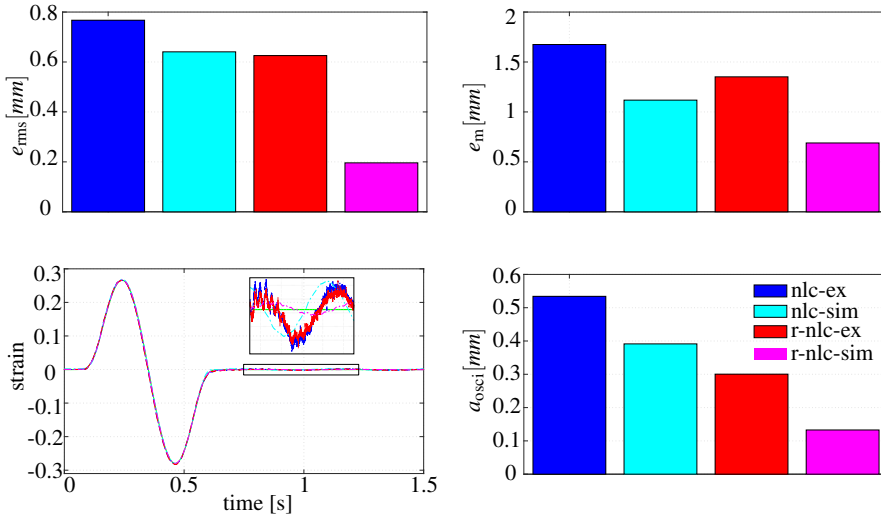


Fig. 4 Comparing root-mean-square (e_{rms}) and maximum(e_m) error during tracking the line trajectory as well as the strain gauge results of the long link and the maximum oscillation amplitude (a_{osci}) at the end-point of the trajectory using two controllers, i.e., the nonlinear controller (nlc) and the reduced nonlinear controller (r-nlc) in experimental test (-ex) on the robot and in simulation (-sim).

For the second scenario, the end-effector shall track an eight shape trajectory. The goal is to validate the tracking performance of the proposed controller in a long more complicated nonlinear trajectory and the trajectory corners. Therefore,

the robot end-effector shall track this trajectory with a length of 0.943 m and with a maximum velocity of 1.03 m/s . In this task, the end-effector tracks the eight shape trajectory that is described with its center/start/end point $x_c = [-0.7, -0.3]^T\text{ m}$. The position of the eight shape points are defined with $[a\sin(2\phi), -a\sin(\phi)]^T$ where $a = 0.1\text{ m}$ and the angle $\phi = [\pi, 3\pi]$. For this scenario, the movie is recorded with approximately 150 frame per second since the recorded area is bigger than the first scenario. The simulation and experiment results are shown in Figure 5.

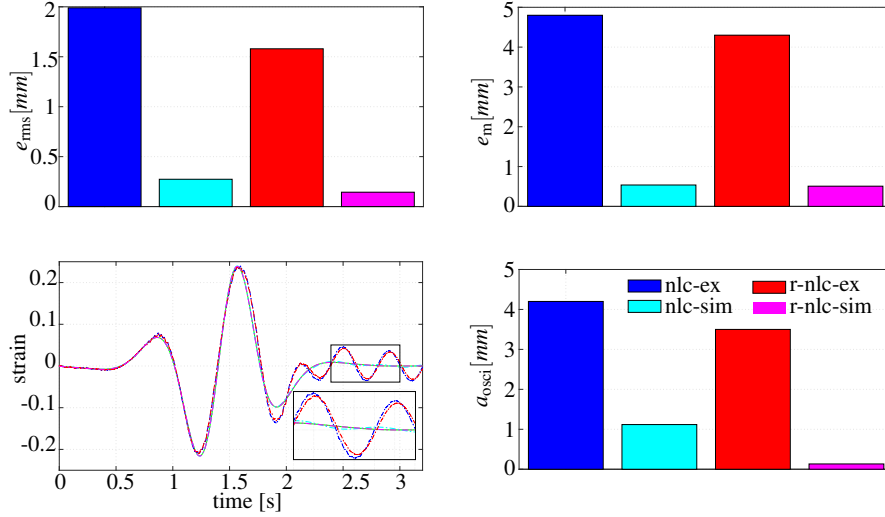


Fig. 5 Comparing the results of two controllers for tracking the eight shape trajectory.

The simulation results on the lambda robot model and the experimental test on the real system show that the presented controller in this paper is able to track a trajectory with high accuracy and high performance. Also, in comparison with the previous work, the tracking performance of the controller in simulation and the experimental test is improved. The presented reduced nonlinear controller reduces the root-mean-square (e_{rms}) and the maximum (e_m) trajectory tracking error at the minimum 21% and 11%, respectively. Also, at the end point, the oscillation amplitude (a_{osci}) is decreased at the minimum 17% in simulation and experimental tests that are shown in Figures 4 and 5.

Conclusions

In this paper, a nonlinear feedback controller was designed based on the reduced model of a flexible parallel lambda shape robot. The controller is tested on the lambda robot in simulation and experiment. The nonlinear feedback controller ob-

tains the robot inputs based on the measurable system states and the desired signals. The controller computes the system inputs based on the direct Lyapunov method. The experiment results for the very flexible parallel robot show that the controller successfully tracks the desired trajectories with high accuracy. Also, experimental validation results demonstrate that the tracking error and the oscillation amplitude of the presented controller are decreased in comparison with the previous works. For future work, the used method and designed controller will be utilized to control the lambda robot's end-effector interaction with an environment using force feedback.

Acknowledgements This research is endorsed by the Cluster of Excellence in Simulation Technology SimTech at the University of Stuttgart and is partially funded by the Landesgraduationkolleg Baden Württemberg. The authors appreciate these discussions.

References

1. Ansarieshlaghi, F. and Eberhard, P. (2017). Design of a nonlinear observer for a very flexible parallel robot. In Proceedings of the 7th GACM Colloquium on Computational Mechanics for Young Scientists from Academia and Industry, Stuttgart, Germany.
2. Ansarieshlaghi, F. and Eberhard, P. (2018). Trajectory tracking control of a very flexible robot using a feedback linearization controller and a nonlinear observer. In Proceedings of 22nd CISM IFToMM Symposium on Robot Design, Dynamics and Control, Rennes, France.
3. Ansarieshlaghi, F. and Eberhard, P. (2018). Experimental study on a nonlinear observer application for a very flexible parallel robot. *International Journal of Dynamics and Control*, doi:10.1007/s40435-018-0467-2.
4. Ansarieshlaghi, F. and Eberhard, P. (2019). Hybrid force/position control of a very flexible parallel robot manipulator in contact with an environment. In Proceedings of 16th International Conference on Informatics in Control, Automation and Robotics. Prague, Czech Republic (submitted).
5. Burkhardt, M., Holzwarth, P., Seifried, R. (2013). Inversion based trajectory tracking control for a parallel kinematic manipulator with flexible links. Proceedings of the 11th International Conference on Vibration Problems. Lisbon, Portugal.
6. Burkhardt, M., Seifried, R., and Eberhard, P. (2014). Experimental studies of control concepts for a parallel manipulator with flexible links. Proceedings of the 3rd Joint International Conference on Multibody System Dynamics and the 7th Asian Conference on Multibody Dynamics, Busan, Korea.
7. Fetić, A, Jurić, D., Osmanković, D. (2012). The procedure of a camera calibration using Camera Calibration Toolbox for MATLAB. Proceedings of the 35th International Convention MIPRO. Opatija, Croatia.
8. Kalil, H.K. (2002). *Nonlinear Systems*, 3rd edition, Prentice-Hall, Upper Saddle River.
9. Morlock, M., Burkhardt, M., Seifried, R. (2015). Friction compensation, gain scheduling and curvature control for a flexible parallel kinematics robot. Proceedings of the 2015 IEEE/RSJ International Conference on Intelligent Robots and Systems, Hamburg, Germany.